

# Molecular Orbital Studies of the Structures and Reactions of Singly Charged Magnesium Ion with Water Clusters, $\text{Mg}^+(\text{H}_2\text{O})_n$

Hidekazu Watanabe,<sup>†,‡</sup> Suehiro Iwata,<sup>\*,†,§</sup> Kenro Hashimoto,<sup>||</sup>  
Fuminori Misaizu,<sup>§</sup> and Kiyokazu Fuke<sup>§</sup>

Contribution from the Department of Chemistry, Faculty of Science and Technology, Keio University, Hiyoshi, Kohoku, Yokohama 223, Japan, Graduate University for Advanced Studies, Myodaiji, Okazaki 444, Japan, Institute for Molecular Science, Myodaiji, Okazaki 444, Japan, and Computer Center, Tokyo Metropolitan University, 1-1 Minami Ohsawa, Hachioji 192-03, Japan

Received August 1, 1994<sup>⊗</sup>

**Abstract:** With ab initio molecular orbital calculations, the structures of the cation clusters  $\text{Mg}^+(\text{H}_2\text{O})_n$  and their hydrogen-eliminated products  $(\text{MgOH})^+(\text{H}_2\text{O})_{n-1}$  are optimized. In  $\text{Mg}^+(\text{H}_2\text{O})_n$ , the hydration number of the most stable isomer is 3. In  $(\text{MgOH})^+(\text{H}_2\text{O})_{n-1}$ , all water molecules are directly bonded to  $\text{Mg}^+$  for  $n \leq 6$ . The hydration energy of  $(\text{MgOH})^+$  is larger than that of  $\text{Mg}^+$  because of the strongly polarized  $(\text{MgOH})^+$  molecular ion; Mg is oxidized halfway to Mg(II). The internal energy change of the hydrogen elimination of  $\text{Mg}^+(\text{H}_2\text{O})_n$  is positive for  $n = 1-5$ , but becomes negative for  $n = 6$ , which is in good agreement with the product switching in the TOF spectrum reported in the preceding paper by Sanekata et al. The effects of isotope substitution and equilibrium constants of the hydrogen (deuterium) elimination reaction observed in their experiment can be explained qualitatively.

## Introduction

Recently, numerous experimental and theoretical studies on the metal–water clusters  $\text{M}(\text{H}_2\text{O})_n$  and their ions  $\text{M}^s(\text{H}_2\text{O})_n$  have been reported. In particular, the detailed experimental studies of the clusters of an atom of the group 1, 2, and 3 elements with water molecules have been reported.<sup>1–15</sup> In these experimental studies, the yield spectra of the photoionization and photochemical reaction of the clusters were examined with the combination of time-of-flight (TOF) and laser spectroscopies.

The structures of these clusters, however, are difficult to determine experimentally. The ab initio molecular orbital method can play an essential role in determining the geometrical structures of the clusters. There are also many theoretical studies on these subjects reported with the ab initio molecular orbital method. In the second period atoms, Hashimoto, Iwata, and their co-workers investigated beryllium and water clusters and their 1+ and 2+ cations.<sup>16–18</sup> Bauschlicher and his co-workers studied sodium, magnesium, and aluminum cation clusters with water molecules ( $\text{Na}^+(\text{H}_2\text{O})_n$ ,  $\text{Mg}^+(\text{H}_2\text{O})_n$ , and  $\text{Al}^+(\text{H}_2\text{O})_n$  up to  $n = 4$ ).<sup>19–25</sup> Hashimoto, He, and Morokuma examined the clusters of a neutral sodium atom with water molecules ( $\text{Na}(\text{H}_2\text{O})_n$ ).<sup>26–28</sup>

Very recently, we studied the structures, stabilities, and reactions of aluminum water clusters  $\text{Al}(\text{H}_2\text{O})_n$  and their ions  $\text{Al}^+(\text{H}_2\text{O})_n$ .<sup>29</sup> In neutral clusters  $\text{Al}(\text{H}_2\text{O})_n$ , there exist two types of structures. The one is  $[\text{Al}(\text{H}_2\text{O})](\text{H}_2\text{O})_{n-1}$ , in which only one water molecule is directly bonded to an aluminum atom.

\* To whom correspondence should be sent.

<sup>†</sup> Keio University.

<sup>‡</sup> Graduate University for Advanced Studies.

<sup>§</sup> Institute for Molecular Science.

<sup>||</sup> Tokyo Metropolitan University.

<sup>⊗</sup> Abstract published in *Advance ACS Abstracts*, December 15, 1994.

(1) Hertel, I. V.; Hüglin, C.; Nitsch, C.; Schultz, C. P. *Phys. Rev. Lett.* **1991**, *67*, 1767.

(2) Schultz, C. P.; Haugstätter, R.; Tittes, H. U.; Hertel, I. V. *Z. Phys. D: At. Mol. Clusters* **1991**, *10*, 279.

(3) Fuke, K.; Misaizu, F.; Sanekata, M.; Tsukamoto, K.; Iwata, S. *Z. Phys. D: At. Mol. Clusters* **1993**, *26*, 180.

(4) Misaizu, F.; Tsukamoto, K.; Sanekata, M.; Fuke, K. *Chem. Phys. Lett.* **1992**, *188*, 241.

(5) Misaizu, F.; Sanekata, M.; Tsukamoto, K.; Fuke, K.; Iwata, S. *J. Phys. Chem.* **1992**, *96*, 8259.

(6) Misaizu, F.; Tsukamoto, K.; Sanekata, M.; Fuke, K.; Iwata, S. *Z. Phys. D: At. Mol. Clusters* **1993**, *26*, 177.

(7) Shen, M. H.; Winniczek, J. W.; Farrar, J. M. *J. Phys. Chem.* **1987**, *91*, 6447.

(8) Shen, M. H.; Farrar, J. M. *J. Phys. Chem.* **1989**, *93*, 4386.

(9) Shen, M. H.; Farrar, J. M. *J. Chem. Phys.* **1991**, *94*, 3322.

(10) Donnelly, S. G.; Farrar, J. M. *J. Chem. Phys.* **1993**, *98*, 5450.

(11) Schmuttenmaer, C. A.; Quan, J.; Donnelly, S. G.; DeLuca, M. J.; Varley, D. F.; DeLouise, L. A.; Millar, R. J. D.; Farrar, J. M. *J. Phys. Chem.* **1993**, *97*, 3077.

(12) Yeh, C. S.; Willey, K. F.; Robbins, D. L.; Pilgrim, J. S.; Duncan, M. A. *Chem. Phys. Lett.* **1992**, *196*, 233.

(13) Willey, K. F.; Yeh, C. S.; Robbins, D. L.; Pilgrim, J. S.; Duncan, M. A. *J. Chem. Phys.* **1992**, *97*, 8886.

(14) Willey, K. F.; Yeh, C. S.; Robbins, D. L.; Duncan, M. A. *J. Phys. Chem.* **1992**, *96*, 7833.

(15) Harms, A. C.; Khanna, S. N.; Chen, B.; Castleman, A. W., Jr. *J. Chem. Phys.* **1994**, *100*, 3540.

(16) Hashimoto, K.; Yoda, N.; Iwata, S. *Chem. Phys.* **1987**, *116*, 193.

(17) Hashimoto, K.; Iwata, S. *J. Phys. Chem.* **1989**, *93*, 2165.

(18) Hashimoto, K.; Yoda, N.; Osamura, Y.; Iwata, S. *J. Am. Chem. Soc.* **1990**, *112*, 7189.

(19) Bauschlicher, C. W., Jr.; Partridge, H. *Chem. Phys. Lett.* **1991**, *181*, 129.

(20) Sodupe, M.; Bauschlicher, C. W., Jr. *Chem. Phys. Lett.* **1991**, *181*, 321.

(21) Bauschlicher, C. W., Jr.; Langhoff, S. F.; Partridge, H.; Rice, J. E.; Komornicki, A. *J. Chem. Phys.* **1991**, *95*, 5142.

(22) Bauschlicher, C. W., Jr.; Partridge, H. *J. Phys. Chem.* **1991**, *95*, 3946.

(23) Bauschlicher, C. W., Jr.; Partridge, H. *J. Phys. Chem.* **1991**, *95*, 9694.

(24) Sodupe, M.; Bauschlicher, C. W., Jr.; *Chem. Phys. Lett.* **1992**, *195*, 494.

(25) Bauschlicher, C. W., Jr.; Sodupe, M.; Partridge, H. *J. Chem. Phys.* **1992**, *96*, 4453.

(26) Hashimoto, K.; He, S.; Morokuma, K. *Chem. Phys. Lett.* **1993**, *206*, 297.

(27) Hashimoto, K.; Morokuma, K. *Chem. Phys. Lett.*, in press.

(28) Hashimoto, K.; Morokuma, K. *J. Am. Chem. Soc.*, submitted.

(29) Watanabe, H.; Aoki, M.; Iwata, S. *Bull. Chem. Soc. Jpn.* **1993**, *66*, 3245.

We call this type the monomer-core structure. The other is  $[\text{Al}(\text{H}_2\text{O})_2](\text{H}_2\text{O})_{n-2}$ , in which two water molecules are directly bonded to an aluminum atom. We call this type the dimer-core structure. The monomer-core structures are always more stable than the dimer-core structures because the hydrogen bonding between two water molecules is stronger than the bonding of the aluminum and water molecule.<sup>29</sup> In the cation clusters  $\text{Al}^+(\text{H}_2\text{O})_n$ , three water molecules can be directly bonded to aluminum cation  $\text{Al}^+$ . In  $\text{Al}^+(\text{H}_2\text{O})_4$ , the fourth water molecule is bonded to two water molecules of the first shell waters. As a result,  $\text{Al}^+(\text{H}_2\text{O})_4$  has a six-membered ring which is very stable.<sup>29</sup> Sodupe and Bauschlicher, Jr. also found a similar structure in  $\text{Al}^+(\text{H}_2\text{O})_4$ .<sup>20</sup>  $\text{Al}^+(\text{H}_2\text{O})_5$  has two types of rings. One is a six-membered ring which is similar to  $\text{Al}^+(\text{H}_2\text{O})_4$ . The other is a larger eight-membered ring. To make this eight-membered ring, the six-membered ring is substantially deformed from a planar structure.

In the preceding paper, the TOF studies of the clusters of the magnesium cation  $\text{Mg}^+$  and water are reported by Sanekata, Misaizu, Fuke, Iwata, and Hashimoto.<sup>30,31</sup> They observed the products of the hydrogen elimination reaction  $(\text{MgOH})^+(\text{H}_2\text{O})_{n-1}$  as well as the water clusters  $\text{Mg}^+(\text{H}_2\text{O})_n$ . In  $n \leq 5$ , the magnesium cation and water clusters  $\text{Mg}^+(\text{H}_2\text{O})_n$  are mostly observed. But in  $6 \leq n \leq 14$ , the cluster ions lacking a hydrogen atom,  $(\text{MgOH})^+(\text{H}_2\text{O})_{n-1}$ , are dominantly observed. In  $n \geq 15$ ,  $\text{Mg}^+(\text{H}_2\text{O})_n$  are the main product again.

Similar experiments are performed with deuterium water clusters  $\text{Mg}^+(\text{D}_2\text{O})_n$ . The product-switching  $n$  has a small isomer effect.

Very recently, Harms, Khanna, Chen, and Castleman, Jr. also reported the experimental studies of  $\text{Mg}^+(\text{H}_2\text{O})_n$  and  $\text{Mg}^+(\text{D}_2\text{O})_n$  clusters.<sup>15</sup> They also found similar hydrogen elimination in larger clusters, and they also carried ab initio calculations to explain the experimental results.

In the present study, the structures of the magnesium–water clusters  $\text{Mg}^+(\text{H}_2\text{O})_n$  and  $(\text{MgOH})^+(\text{H}_2\text{O})_{n-1}$  ( $n = 1-6$ ) are determined with the ab initio molecular orbital method. We first discuss the structures and stabilities of  $\text{Mg}^+(\text{H}_2\text{O})_n$  and  $(\text{MgOH})^+(\text{H}_2\text{O})_{n-1}$ . The role of molecular ion  $(\text{MgOH})^+$  is examined. Then, the hydration energies of  $\text{Mg}^+(\text{H}_2\text{O})_n$  and  $(\text{MgOH})^+(\text{H}_2\text{O})_{n-1}$  are evaluated. On the basis of the change of the hydration energies, we elucidate the hydrogen elimination reaction of  $\text{Mg}^+(\text{H}_2\text{O})_n$  and analyze the experimental findings in the preceding paper.<sup>31</sup>

## Method

The geometrical structures of the magnesium cation–water clusters  $\text{Mg}^+(\text{H}_2\text{O})_n$  and  $(\text{MgOH})^+(\text{H}_2\text{O})_{n-1}$  ( $n = 1-6$ ) are optimized with the unrestricted self-consistent-field (UHF) and closed shell restricted self-consistent-field (RHF) methods. To confirm the true stability, the harmonic frequencies at the optimized structures are evaluated. For  $n = 1$  and  $n = 2$  of each set of clusters, the structures are reoptimized with the second-order Møller–Plesset (MP2) method to examine the effect of the electron correlation on the Mg–O distance. The basis set used in the optimization is 6-31G. Geometrical parameters of all isomers for  $n \leq 3$  and those of the most stable isomers for  $n \geq 4$  obtained with 6-31G basis set are refined with the 6-31G\* basis set. The hydrogen elimination reaction energies of  $\text{Mg}^+(\text{H}_2\text{O})_n$  and hydration energies of  $\text{Mg}^+(\text{H}_2\text{O})_n$  and  $(\text{MgOH})^+(\text{H}_2\text{O})_{n-1}$  are evaluated with MP2 and MP4SDTQ levels at the optimized structures of SCF levels of 6-31G and 6-31G\* basis sets. The hydrogen elimination and hydration energies are corrected by adding the zero-point vibration energies. The programs used are GAUSSIAN88<sup>32</sup> and GAUSSIAN92.<sup>33</sup> GAUSSIAN

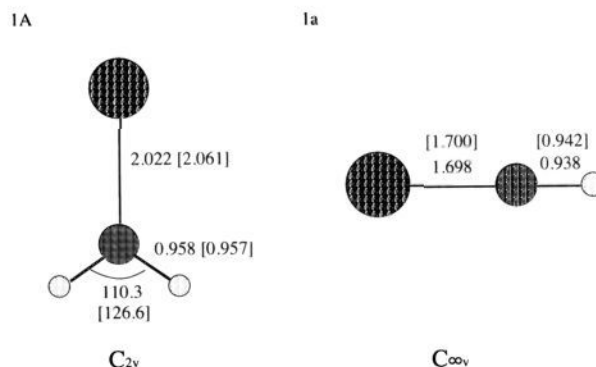


**Figure 1.** Optimized structures of  $\text{Mg}^+(\text{H}_2\text{O})$  (1A) and of  $(\text{MgOH})^+$  (1a). The geometrical parameters are determined with the SCF/6-31G [SCF/6-31G\*] method. In the following figures, the true stabilities of the optimized structures are confirmed by evaluating the harmonic frequencies.

AN88 is registered at the computer center of the Institute for Molecular Science (IMS). The computations were carried out on S820 at IMS and on our workstations.

To analyze the product distribution of the preceding paper,<sup>31</sup> the equilibrium constants of the hydrogen elimination reaction are evaluated using the harmonic frequencies calculated with the SCF method.

## Results and Discussion

**A. Structures of  $\text{Mg}^+(\text{H}_2\text{O})_n$ .** The optimized structures of  $\text{Mg}^+(\text{H}_2\text{O})_n$  ( $n = 1-6$ ) clusters are shown in Figures 1–6. The values under the figures are the relative energies in kilojoules per mole among the isomers; they are evaluated with the SCF/6-31G//SCF/6-31G (MP4SDTQ/6-31G\*\*//SCF/6-31G\*) method. The maximum expectation values of  $S^2$  in the UHF wave function are 0.7504 in the 6-31G basis and 0.7503 in the 6-31G\* basis.

Figure 1 shows the structure of  $\text{Mg}^+(\text{H}_2\text{O})$  (1A). The four atoms lie on a plane, and the complex has  $C_{2v}$  symmetry. Most of the geometrical parameters of each structure are hereafter given in the figure (full geometrical parameters will be distributed on request through e-mail).<sup>34</sup> The parameters without brackets are evaluated at the SCF/6-31G level and in brackets are evaluated at the SCF/6-31G\* level. There is little difference between the two basis sets. The polarization functions do not affect the optimized structure of  $\text{Mg}^+(\text{H}_2\text{O})$  very much. Table 1 compares the geometrical parameters between SCF and MP2 methods with 6-31G basis sets. There is also little difference between the parameters of the SCF and MP2 methods.

Figure 2 shows the structures of  $\text{Mg}^+(\text{H}_2\text{O})_2$ . Two types of isomers are found in  $\text{Mg}^+(\text{H}_2\text{O})_2$ . Structure 2A has two water molecules directly bonded to a magnesium atom. The bond angle of O–Mg–O is nearly  $90^\circ$ . The two water molecules are staggered (see the side view), and the cluster has  $C_2$  symmetry. Structure 2B has only one water directly bonded to the magnesium atom, and the second water is bound to the first water through a hydrogen bond. The polarization functions do not have a large effect on the structures  $\text{Mg}^+(\text{H}_2\text{O})_2$  except for the distance of  $\text{H}_2\text{O}-\text{H}_2\text{O}$  hydrogen bonding. The electronic

(32) Frisch, M. J.; Head-Gordon, M.; Schlegel, H. B.; Raghavachari, K.; Binkley, J. S.; Gonzalez, C.; Defrees, D. J.; Fox, D. J.; Whiteside, R. A.; Seeger, R.; Melius, C. F.; Baker, J.; Martin, R. L.; Khan, L. R.; Stewart, J. J. P.; Fluder, E. M.; Topoil, S.; Pople, J. A. *GAUSSIAN 88*; Gaussian, Inc.: Pittsburgh, PA, 1988.

(33) Frisch, M. J.; Trucks, G. W.; Head-Gordon, M.; Gill, P. M. W.; Wong, M. W.; Foresman, J. B.; Johnson, B. G.; Schlegel, H. B.; Robb, M. A.; Replogle, E. S.; Gomperts, R.; Andres, J. L.; Raghavachari, K.; Binkley, J. S.; Gonzalez, C.; Martin, R. L.; Fox, D. J.; Defrees, D. J.; Baker, J.; Stewart, J. J. P.; Pople, J. A. *GAUSSIAN 92*, Revision E.2; Gaussian, Inc.: Pittsburgh, PA, 1992.

(34) E-mail address: iwata@ims.ac.jp.

(30) Misaizu, F.; Sanekata, M.; Fuke, K.; Iwata, S. *J. Chem. Phys.* **1994**, *100*, 1161.

(31) Sanekata, M.; Misaizu, F.; Fuke, K.; Iwata, S.; Hashimoto, H. *J. Am. Chem. Soc.* **1995**, *116*, 747.

**Table 1.** Geometrical Parameters of  $\text{Mg}^+(\text{H}_2\text{O})_n$  and  $(\text{MgOH})^+(\text{H}_2\text{O})_{n-1}$  ( $n \leq 2$ ) by the SCF and MP2 Methods<sup>a</sup>

		SCF	MP2
$\text{Mg}^+(\text{H}_2\text{O})$	Mg–O	2.022	2.043
	O–H	0.958	0.980
	H–O–H	110.3	109.6
$(\text{MgOH})^+$	Mg–O	1.698	1.785
	O–H	0.938	0.960
$\text{Mg}^+(\text{H}_2\text{O})_2$ (2A)	Mg–O	2.044	2.064
	O–H	0.955	0.978
		0.956	0.979
$\text{Mg}^+(\text{H}_2\text{O})_2$ (2B)	O–Mg–O	94.1	94.6
	H–O–H	110.9	110.0
	Mg–O(1)	1.965	1.983
	O(1)–H(a)	0.954	0.976
	O(1)–H(b)	0.995	1.025
	H(b)–O(2)	1.574	1.544
$(\text{MgOH})^+(\text{H}_2\text{O})$ (2a)	O(2)–H	0.952	0.974
	H(a)–O(1)–H(b)	110.9	110.7
	Mg–O(0)	1.712	1.727
	O(0)–H	0.937	0.959
	Mg–O(1)	1.961	1.984
	O(1)–H	0.958	0.979
$(\text{MgOH})^+(\text{H}_2\text{O})$ (2b)		0.959	0.980
	O(0)–Mg–O(1)	171.2	171.1
	H–O(1)–H	110.0	109.5
	Mg–O(0)	1.692	1.714
	O(0)–H(a)	0.957	0.990
	H(a)–O(1)	1.760	1.666
	O(1)–H	0.950	0.973
Mg–O(0)–H(a)	180.0	180.0	
H–O(1)–H	112.0	110.8	

<sup>a</sup> The basis set used is 6-31G. The numbering of atoms are given in Figures 1 and 2. Bond lengths and angles are in angstroms and degrees.

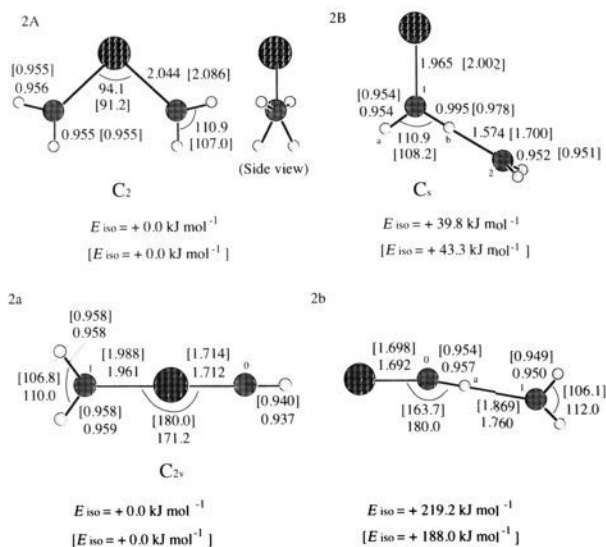


**Figure 2.** Optimized structures of  $\text{Mg}^+(\text{H}_2\text{O})_2$  (2A,B) and  $(\text{MgOH})^+(\text{H}_2\text{O})$  (2a,b). The structures are optimized with the SCF/6-31G [SCF/6-31G\*] method. The energy  $E_{\text{iso}}$  is evaluated with the SCF/6-31G/SCF/6-31G [MP4SDTQ/6-31G\*\*/SCF/6-31G\*] method. The side view is shown in  $\text{Mg}^+(\text{H}_2\text{O})_2$  (2A).

correlation, taken into account with the MP2 method, does not affect the optimized structures very much for both of the isomers (see Table 1). It implies that the bond between the Mg and O atoms is mostly electrostatic. Besides, structure 2A suggests the weak covalency of a nonbonding orbital of water oxygen coordinating to a vacant  $3p_{(\text{Mg})}$  atomic orbital of Mg.

The second hydration changes the geometry of the first shell. One of the O–H bonds of the first shell water, which is bonded to the second shell water, is longer than the other. For example,

**Table 2.** Gross Mulliken Populations of Mg, O, and H Atoms in  $\text{Mg}^+(\text{H}_2\text{O})_n$ <sup>a</sup>

	H <sub>2</sub> O without the second shell			H <sub>2</sub> O with the second shell		
	Mg	O	H	O	H	
1	+0.879	−0.941	+0.531	+0.531		
2A	+0.785	−0.935	+0.525	+0.518		
		−0.935	+0.525	+0.518		
2B	+0.851	−0.920	+0.487	+0.487	−1.011	+0.519 +0.588 <sup>a</sup>
3A	+0.702	−0.930	+0.518	+0.511		
		−0.930	+0.518	+0.511		
		−0.930	+0.518	+0.511		
3B	+0.772	−0.921	+0.491	+0.491	−0.977	+0.517 +0.544 <sup>b</sup>
					−0.977	+0.517 +0.544 <sup>b</sup>
4	+0.689	−0.925	+0.517	+0.505	−0.967	+0.509 +0.537 <sup>b</sup>
		−0.917	+0.487	+0.487	−0.967	+0.509 +0.537 <sup>b</sup>
5	+0.692	−0.909	+0.482	+0.482	−0.966	+0.508 +0.531 <sup>b</sup>
				−0.966	+0.508 +0.531 <sup>b</sup>	
				−0.973	+0.507 +0.538 <sup>b</sup>	
				−0.952	+0.479 +0.506 <sup>b</sup>	
6	+0.660	−0.908	+0.471	+0.471	−0.995	+0.495 +0.581 <sup>b</sup>
		−0.907	+0.474	+0.474	−0.971	+0.502 +0.542 <sup>b</sup>
				−0.971	+0.502 +0.542 <sup>b</sup>	
				−0.978	+0.473 +0.544 <sup>b</sup>	

<sup>a</sup> The basis set used is 6-31G\*. <sup>b</sup> Bonded to an O atom in the second shell.

at the SCF/6-31G\* level, the bond length O(1)–H(b) of 2B is 0.978 Å, and O(1)–H(a) and O(2)–H of 2B and O–H of 2A are 0.954, 0.951, and 0.955 Å, respectively. Besides, the second hydration makes the bond length of Mg–O short. At the SCF/6-31G\* level, the Mg–O distance in 2B is 2.002 Å, whereas that in 2A is 2.086 Å. The second hydration has also an effect on the Mulliken population of the atoms in the first shell. Table 2 shows the gross Mulliken population of all atoms in  $\text{Mg}^+(\text{H}_2\text{O})_n$ . The values shown in the right-hand side are for the hydrogen atoms which are bonded to an oxygen atom of the second shell water via a hydrogen bond. The Mulliken population of the latter hydrogens is more positive than that of the other hydrogens. The oxygen atoms of the proton acceptor are more negative than the other oxygens. In other words, the water molecules are more polarized by the hydrogen bonds. These characteristics are seen in all clusters  $\text{Mg}^+(\text{H}_2\text{O})_n$  having the second (and more) hydration shell. In the neutral and cation aluminum–water clusters  $\text{Al}(\text{H}_2\text{O})_n$  and  $\text{Al}^+(\text{H}_2\text{O})_n$ , we also found a similar tendency in bond lengths and in Mulliken population by the second hydration.<sup>29</sup>

The difference in the isomerization energies  $E_{\text{iso}}$  between two calculation levels is not significant. Structure 2A is more stable than structure 2B. In other words, the  $\text{Mg}^+\text{–OH}_2$  bond is stronger than the hydrogen bond of  $\text{H}_2\text{O}\text{–H}_2\text{O}$ .

The structures of  $\text{Mg}^+(\text{H}_2\text{O})_3$  are given in Figure 3. Two types of isomers are found for  $\text{Mg}^+(\text{H}_2\text{O})_3$ . The most stable structure is structure 3A of C<sub>3</sub> symmetry, in which three water molecules are directly bonded to  $\text{Mg}^+$  cation. Another isomer is structure 3B of C<sub>s</sub> symmetry, in which the third water molecule is bonded to the water molecules of the first shell via two hydrogen bonds. This structure has a six-membered ring which stabilizes the complex. The total energy of 3B is higher than that of 3A by 14.4 kJ mol<sup>−1</sup>. Among the isomers of  $\text{Mg}^+(\text{H}_2\text{O})_3$ , the structure in which only one water molecule is directly bonded to a magnesium might be possible. But, because of the relative stability of the two isomers 2A,B, we can deduce that such a structure is less stable than 3A,B.

Structures of  $\text{Mg}^+(\text{H}_2\text{O})_4$  are shown in Figure 4. The structure 4A has a six-membered ring. Three water molecules make a six-membered ring structure as in structure 3B of  $\text{Mg}^+(\text{H}_2\text{O})_3$ , and the fourth water molecule is directly bonded

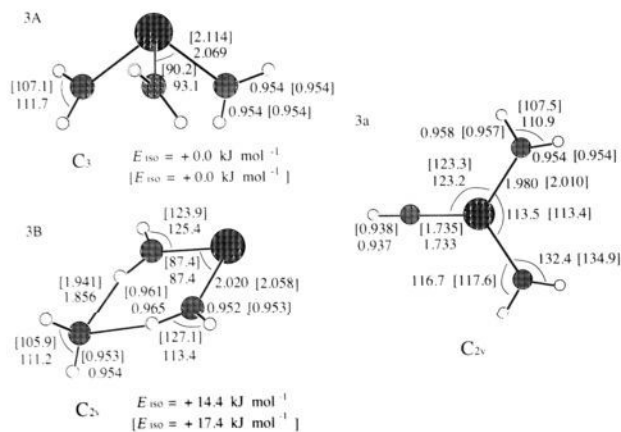


**Figure 3.** Optimized structures of  $\text{Mg}^+(\text{H}_2\text{O})_3$  (3A,B) and  $(\text{MgOH})^+(\text{H}_2\text{O})_2$  (3a). The structures are optimized with the SCF/6-31G [SCF/6-31G\*] method. The energy  $E_{\text{iso}}$  is evaluated with the SCF/6-31G//SCF/6-31G [MP4SDTQ/6-31G\*\*/SCF/6-31G\*] method.

to the magnesium atom. In structure 4A, the number of waters which are directly bonded to a magnesium atom is three. The isomer 4B has also a six-membered ring which is similar to structure 3B. The fourth water molecule of structure 4B is not directly bonded to the magnesium atom but bonded to the water molecule which closes the six-membered ring. In structure 4B, the number of waters which are directly bonded to the magnesium atom is two. In the third isomer of  $\text{Mg}^+(\text{H}_2\text{O})_4$ , 4C, all four water molecules are directly bonded to a magnesium atom. The symmetry of structure 4C is  $C_{2v}$ . The most stable structure of  $\text{Mg}^+(\text{H}_2\text{O})_4$  is 4A. The second and the third stable structures are 4C,B at the SCF/6-31G level. But, the energy difference between 4C and 4B is very small.

For  $n = 1-4$ , the structures of  $\text{Mg}^+(\text{H}_2\text{O})_n$  are very similar to the structures of  $\text{Al}^+(\text{H}_2\text{O})_n$ .<sup>29</sup> In contrast to the isomers of  $\text{Mg}^+(\text{H}_2\text{O})_3$  and  $\text{Mg}^+(\text{H}_2\text{O})_4$ , our recent study of  $\text{Al}^+(\text{H}_2\text{O})_4$  shows that the isomers having three waters directly bonding to the central ion (3A and 4A type) are less stable than the other isomers having the hydrogen-bonding ring (3B and 4B type).<sup>35</sup> The difference of the most stable isomer in  $\text{Mg}^+$ - and  $\text{Al}^+$ -water clusters results from the binding energy difference of the bonds between the metal-water and water-water. At the MP2/6-31G\*\*/SCF/6-31G\* level, the hydration energy of  $\text{Mg}^+(\text{H}_2\text{O})$  is 1.725 eV, while that of  $\text{Al}^+(\text{H}_2\text{O})$  is 1.466 eV.<sup>35</sup> The stabilization due to the six-membered ring is larger than that of  $\text{Al}^+-\text{H}_2\text{O}$  bond formation.

In  $\text{Mg}^+(\text{H}_2\text{O})_4$ , there is an isomer whose hydration number is four (structure 4C), while in  $\text{Al}^+(\text{H}_2\text{O})_4$ , however, we could not locate the isomer of structure 4C type.<sup>29</sup> The bond lengths of the magnesium ion-water are shorter than those of the aluminum ion-water in the same cluster size  $n$ . Consequently, the distances of the two water molecules become close to each other and four water molecules in  $\text{Mg}^+(\text{H}_2\text{O})_4$  can be bonded with a weak hydrogen bonding and make a hydrogen-bonding network. The length of this hydrogen bonding is 2.769 Å and is shown with dotted lines in Figure 4C. In  $\text{Al}^+(\text{H}_2\text{O})_4$ , the bond lengths of aluminum and water are too long to make a network similar to that of  $\text{Mg}^+(\text{H}_2\text{O})_4$ .<sup>29</sup> A similar, but stronger, network of  $(\text{H}_2\text{O})_4$  was found in  $\text{Na}(\text{H}_2\text{O})_4$  by Hashimoto et al. (see refs 26-28).

Sodupe and Bauschlicher<sup>19,23,25</sup> previously determined the structures of  $\text{Mg}^+(\text{H}_2\text{O})_n$  and  $\text{Al}^+(\text{H}_2\text{O})_n$  for  $n \leq 4$ . Our structures are very similar to theirs, but in  $\text{Mg}^+(\text{H}_2\text{O})_4$ , their structure corresponding to our 4C has  $C_2$  symmetry. The

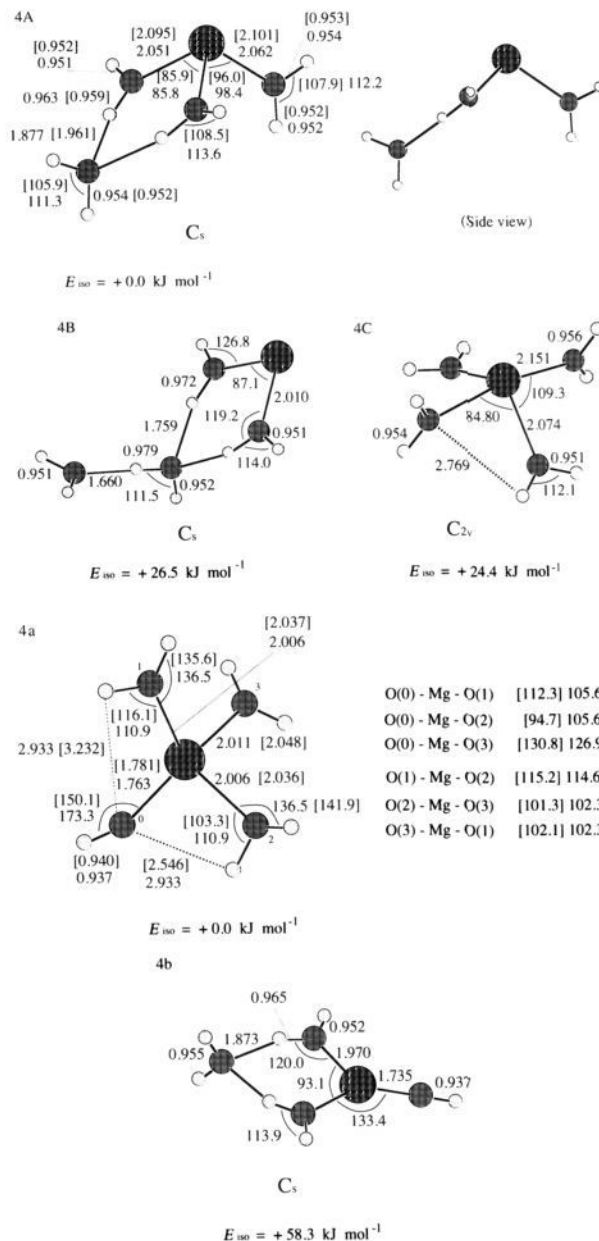


**Figure 4.** Optimized structures of  $\text{Mg}^+(\text{H}_2\text{O})_4$  (4A,B,C) and  $(\text{MgOH})^+(\text{H}_2\text{O})_3$  (4a,b). The structures are optimized with the SCF/6-31G [SCF/6-31G\*] method. The energy  $E_{\text{iso}}$  is evaluated with the SCF/6-31G method. The right picture of structure 4A is a side view of the cluster.

isomerization energies are 14.4  $\text{kJ mol}^{-1}$  for  $n = 3$  and 24.4  $\text{kJ mol}^{-1}$  for  $n = 4$  in our calculation and 17  $\text{kJ mol}^{-1}$  for  $n = 4$  with the SCF/TZ2P//SCF/6-31G\* level of approximation in Bauschlicher and Partridge.

Experimentally, photodissociation yield spectra of  $\text{Mg}^+(\text{H}_2\text{O})_n$  are obtained by Misaizu et al.<sup>30</sup> The yield spectra of  $\text{Mg}^+(\text{H}_2\text{O})_n$  for  $n = 1-3$  shift gradually to low energy with increasing cluster size  $n$ . For  $n = 4$  and 5, the small red shifts of the spectra from  $n = 3$  were observed. We can deduce that the hydration number of the most stable structures of  $\text{Mg}^+(\text{H}_2\text{O})_n$  is saturated at  $n = 3$ , and that the second hydration shell is formed at  $n \geq 4$ , from the similarity of the photodissociation spectra of  $n = 3$  and  $n = 4$ .

Harms et al. reported the structures in which all water molecules are directly bonded to magnesium from  $n = 1$  to  $n = 6$ .<sup>15</sup> But, as shown above, the stability among the isomers

(35) Watanabe, H.; Nakamura, H.; Iwata, S. manuscript in preparation.



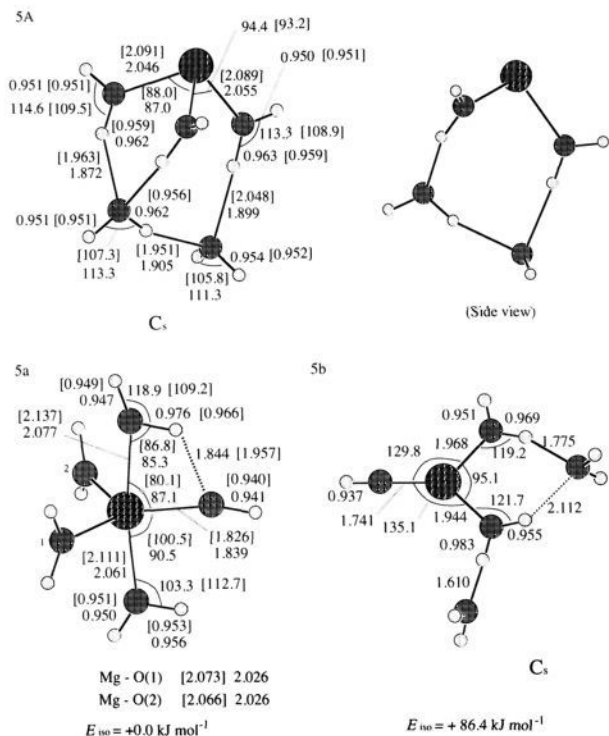


**Figure 5.** Optimized structures of  $\text{Mg}^+(\text{H}_2\text{O})_5$  (5A) and  $(\text{MgOH})^+(\text{H}_2\text{O})_4$  (5a,b). The structures are optimized with the SCF/6-31G [SCF/6-31G\*] method. The energy  $E_{\text{iso}}$  is evaluated with the SCF/6-31G method. The right picture of structure 5A is a side view of the cluster.

of  $n = 3$  and  $n = 4$  strongly suggests that the hydration number of the most stable isomer of  $\text{Mg}^+(\text{H}_2\text{O})_n$  is 3. The hydration number of the most stable isomers of  $\text{Mg}^+(\text{H}_2\text{O})_n$  might be explained by the classical octet rule. If the octet rule is assumed, three water molecules can be directly bonded to  $\text{Mg}^+$  because a magnesium cation  $\text{Mg}^+$  has one valence electron.

Figure 5A shows the structure of  $\text{Mg}^+(\text{H}_2\text{O})_5$ . The hydration number of structure 5A is also 3. There are two types of rings. One is the six-membered ring which is similar to the one in  $\text{Mg}^+(\text{H}_2\text{O})_4$ , and the other is an eight-membered ring. The fifth water molecule is bonded to two water molecules, and it makes the eight-membered ring, which deforms the planarity of the six-membered ring in  $\text{Mg}^+(\text{H}_2\text{O})_5$  (compare the side views of Figure 4A and Figure 5A). We may also have to consider the isomers derived from structures 4B,C. The isomers derived from 4B, except for 5A, cannot form another hydrogen-bonding ring as 5A has. The isomers from 4C can form one ring but not two as 5A does. Therefore, the other isomers are less stable than structure 5A. The most stable isomers of the  $\text{Al}^+(\text{H}_2\text{O})_5$  cluster have a structure very similar to 5A.<sup>29,35</sup>

The structures of  $\text{Mg}^+(\text{H}_2\text{O})_6$  are shown in Figure 6. Only the isomers in which three water molecules are directly bonded to magnesium cation are shown. There are two types of isomers. Structure 6A,  $[\text{Mg}^+(\text{H}_2\text{O})_4](\text{H}_2\text{O})_2$ , has  $\text{Mg}^+(\text{H}_2\text{O})_4$  (4A) as a core, and structure 6B,  $[\text{Mg}^+(\text{H}_2\text{O})_5](\text{H}_2\text{O})$ , has  $\text{Mg}^+(\text{H}_2\text{O})_5$  as a core. The hydrogen bonding, which is shown in a dotted line in structure 6B, is weaker than the others. The bond length is 2.010 Å and longer than the other hydrogen bondings (about 1.7–1.8 Å). Both isomers 6A,B are very close in energy. In both types of structures, a few other isomers are found. All isomers we found are within 10  $\text{kJ mol}^{-1}$  above the most stable structures 6A,B.

**B. Structures of  $(\text{MgOH})^+(\text{H}_2\text{O})_{n-1}$ .** The optimized structures of  $(\text{MgOH})^+(\text{H}_2\text{O})_{n-1}$  ( $n = 1-6$ ) clusters are also shown in Figures 1–6. The values under the figures are the relative

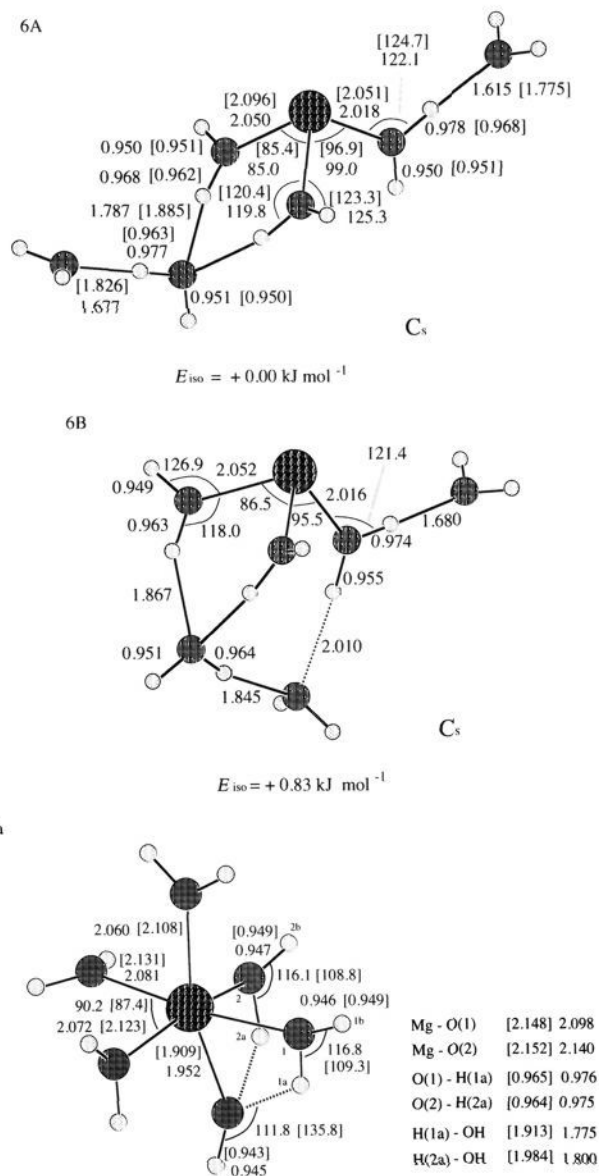


**Figure 6.** Optimized structures of  $\text{Mg}^+(\text{H}_2\text{O})_6$  (6A,B) and  $(\text{MgOH})^+(\text{H}_2\text{O})_5$  (6a). The structures are optimized with the SCF/6-31G [SCF/6-31G\*] method. The energy  $E_{\text{iso}}$  is evaluated with the SCF/6-31G method.

energies in kilojoules per mole among the isomers; they are evaluated with the SCF method.

Figure 1 shows the structure 1a of  $(\text{MgOH})^+$ . The geometrical parameters of each structure are given in the figure; the parameters determined with the SCF/6-31G level are without brackets, and those with the SCF/6-31G\* level are in brackets. The molecular ion  $(\text{MgOH})^+$  is linear and is strongly polarized, which makes the hydration energies become large, as is discussed in the following subsection.

Structures of two types of isomers (2a,b) for  $(\text{MgOH})^+(\text{H}_2\text{O})$  are shown in Figure 2. In structure 2a, both  $\text{H}_2\text{O}$  and  $\text{OH}$  are bound to  $\text{Mg}^+$  directly. These are a small basis set dependence on the optimized structure. In the SCF/6-31G\* level, the frame  $\text{O}(0)-\text{Mg}-\text{O}(1)$  is completely linear and the cluster has  $C_{2v}$  symmetry, while in the SCF/6-31G level,  $\text{O}(0)-\text{Mg}-\text{O}(1)$  is slightly bent and the cluster has  $C_s$  symmetry. In structure 2b, the water molecule is bonded to a hydrogen atom of  $\text{OH}$ . Structure 2b is much less stable than 2a by 219.2  $\text{kJ mol}^{-1}$ . The hydration bond of  $(\text{HOMg})^+-\text{OH}_2$  is much stronger than

**Table 3.** Gross Mulliken Population of Mg, O, and H Atoms in  $(\text{MgOH})^+(\text{H}_2\text{O})_{n-1}$ 

	Mg	in -OH		in H <sub>2</sub> O		
		O	H	O	H	
1	+1.580	-1.072	+0.492			
2a	+1.478	-1.092	+0.479	-0.962	+0.549	+0.548
2b	+1.533	-1.114	+0.551	-0.898	+0.464	+0.464
3	+1.386	-1.077	+0.463	-0.956	+0.529	+0.541
				-0.956	+0.529	+0.541
4	+1.319	-1.079	+0.447	-0.949	+0.540	+0.514
				-0.947	+0.532	+0.520
				-0.944	+0.524	+0.525
5	+1.298	-1.091	+0.438	-0.943	+0.507	+0.518
				-0.965	+0.549 <sup>b</sup>	+0.494
				-0.929	+0.513	+0.511
				-0.932	+0.522	+0.510
6	+1.234	-1.102	+0.437	-0.950	+0.542 <sup>b</sup>	+0.489
				-0.950	+0.537 <sup>b</sup>	+0.492
				-0.923	+0.512	+0.503
				-0.929	+0.508	+0.514
				-0.936	+0.506	+0.513

<sup>a</sup> The basis set used is 6-31G\*. <sup>b</sup> Bonded to an O atom in -OH.

the hydration bond of  $(\text{MgOH})^+-\text{OH}_2$ . Though we located the isomers similar to 2b for  $n \geq 2$ , we found that such structures are much less stable than the most stable isomers.

Figure 3 shows the structure 3a of  $(\text{MgOH})^+(\text{H}_2\text{O})_2$ . An OH group and both water molecules are directly bonded to  $\text{Mg}^+$ . The angles of  $(\text{H}_2\text{O})-\text{Mg}-\text{OH}$  and  $(\text{H}_2\text{O})-\text{Mg}-\text{O}(\text{H}_2)$  are close to  $120^\circ$ , and  $\text{Mg}^+$  and three O atoms lie on a plane. The symmetry of the cluster  $(\text{MgOH})^+(\text{H}_2\text{O})_2$  is  $C_s$ .

Structures (4a,b) of  $(\text{MgOH})^+(\text{H}_2\text{O})_3$  are shown in Figure 4. In structure 4a, all three water molecules are directly bonded to  $(\text{MgOH})^+$ . Four oxygen atoms form nearly  $T_d$  symmetry. In structure 4a, the basis set dependence is also found. With the 6-31G basis, the cluster has  $C_s$  symmetry and  $\text{O}(0)-\text{Mg}-\text{O}(3)$  makes a mirror plane, while with the 6-31G\* basis, the symmetry is slightly broken. Structure 4b has a six-membered ring which is similar to that in structure 3A of  $\text{Mg}^+(\text{H}_2\text{O})_3$ . In spite of a stable six-membered ring, structure 4b is less stable than structure 4a. Previously, Hashimoto and Iwata determined the structures of  $(\text{BeOH})^+(\text{H}_2\text{O})_{n-1}$  for  $n \leq 4$ .<sup>18</sup> The structures of  $(\text{BeOH})^+(\text{H}_2\text{O})_{n-1}$  they determined are all similar to those of the corresponding  $(\text{MgOH})^+(\text{H}_2\text{O})_{n-1}$ .

Figure 5 shows the two isomers of  $(\text{MgOH})^+(\text{H}_2\text{O})_4$ . In structure 5a, all four water molecules are bonded to the  $(\text{MgOH})^+$  molecular ion directly. Structure 5a does not satisfy the classical octet rule, while structure 5b satisfies it, having three waters in the first shell. When the  $\text{Mg}^+$  ion is bonded to an OH radical, only three vacant orbitals are left around the magnesium. Structure 5a with five oxygens in the first shell, however, is the most stable isomer in  $(\text{MgOH})^+(\text{H}_2\text{O})_4$ . As is discussed below, the electrostatic interaction between  $(\text{MgOH})^+$  and water molecules dominates the first shell formation.

The structure of  $(\text{MgOH})^+(\text{H}_2\text{O})_5$  is shown in 6a. In this structure, all five water molecules are directly bonded to the magnesium atom as in structure 5a of  $(\text{MgOH})^+(\text{H}_2\text{O})_4$ .

**Molecular Ion  $(\text{MgOH})^+$ .** As shown above,  $(\text{MgOH})^+$  behaves as a core molecular ion in  $(\text{MgOH})^+(\text{H}_2\text{O})_{n-1}$  clusters, and the hydration of  $(\text{MgOH})^+$  is much larger than that of  $\text{Mg}^+$ .

Table 3 shows the gross Mulliken populations of Mg, O, and H atoms in  $(\text{MgOH})^+(\text{H}_2\text{O})_{n-1}$ . The Mulliken charge of Mg in  $(\text{MgOH})^+$  is between +1.2 and +1.6, and that of O is about -1.1 at the SCF/6-31G\* level. In  $\text{Mg}^+(\text{H}_2\text{O})_n$ , the Mulliken charge of Mg is between +0.6 and +0.9, and that of O is about -0.95. The electron is transferred from Mg to O, and the charge distribution of  $(\text{MgOH})^+$  in the clusters is strongly polarized.

The magnesium atom in  $(\text{MgOH})^+$  is almost oxidized halfway to  $\text{Mg}^{2+}$ . Harms et al. also found the polarization of the  $(\text{MgOH})^+$  molecular ion.<sup>15</sup>

The large hydration energy of  $(\text{MgOH})^+$  results from the strong polarization of the  $(\text{MgOH})^+$  molecular ion. The strong bond between  $(\text{MgOH})^+$  and  $\text{H}_2\text{O}$  is seen also in the bond lengths. For  $n = 4$ , the bond length of  $\text{Mg}-\text{OH}_2$  in  $(\text{MgOH})^+(\text{H}_2\text{O})_{n-1}$  is shorter than that of the most stable isomers of  $\text{Mg}^+(\text{H}_2\text{O})_n$ . For  $n \geq 5$ , this rule no longer holds because of the cloudiness around  $(\text{MgOH})^+$ .

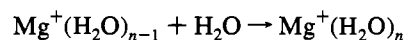
The maximum number of water molecules in the first shell of  $(\text{MgOH})^+(\text{H}_2\text{O})_{n-1}$  for  $n \geq 5$  is also explained by the strong electrostatic coordination of the  $(\text{MgOH})^+$  ion with water molecules. In  $\text{Mg}^+(\text{H}_2\text{O})_n$ , the hydration number in the first shell of the most stable isomers is 3 and satisfies the octet rule. The isomers with more than four waters in the first shell are less stable. On the other hand, the magnesium atoms in the most stable isomers of  $(\text{MgOH})^+(\text{H}_2\text{O})_4$  and  $(\text{MgOH})^+(\text{H}_2\text{O})_5$  are surrounded by five and six oxygen atoms, respectively. The breakdown of the classical octet rule in  $n \geq 5$  results from the strong electrostatic interaction between  $(\text{MgOH})^+$  and water molecules.

Harms et al. found structures which also have all water molecules directly bonded to the  $(\text{MgOH})^+$  molecular ion.<sup>15</sup> But, our structures 5a and 6a have characteristics which differ from the structures of Harms et al. In our structures, an oxygen atom in  $(\text{MgOH})^+$  is bound to a hydrogen atom in one of the water molecules through a hydrogen bond (shown in Figures 5 and 6 with dotted lines). They make a small four-membered ring with the magnesium atom. There is a ring in structure 5a and two rings in structure 6a. The strongly polarized oxygen atom in  $(\text{MgOH})^+$  attracts the hydrogen atom(s) in the neighboring water(s). These rings also stabilize the isomers 5a and 6a.

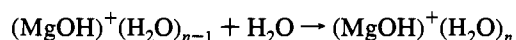
We cannot find the isomer of  $(\text{MgOH})^+(\text{H}_2\text{O})_4$  which has structure 4a as a core. If a water molecule approaches  $(\text{MgOH})^+(\text{H}_2\text{O})_3$  of structure 4a, the water molecule is not bonded to the other water molecules, but bonded directly to the magnesium atom, because the binding energy of  $(\text{MgOH})^+$  and an  $\text{H}_2\text{O}$  molecule is very large!

The hydrogen atom in  $(\text{MgOH})^+$  is less positive than those of  $\text{H}_2\text{O}$  molecules (see Table 3), and therefore, the hydrogen bonding of  $\text{MgOH}-\text{OH}_2$  is weaker than that of  $\text{H}_2\text{O}-\text{H}_2\text{O}$ . In  $(\text{MgOH})^+(\text{H}_2\text{O})$ , structure 2b is much less stable (219.2 kJ mol<sup>-1</sup>) than structure 2a. In  $(\text{MgOH})^+(\text{H}_2\text{O})_2$ , we have examined the structures where the third water molecules are bonded to the hydrogen of OH: such structures are less stable, as is the case for  $(\text{MgOH})^+(\text{H}_2\text{O})$ .

**C. Hydration Energies and Reaction Energies of  $\text{Mg}^+(\text{H}_2\text{O})_n$ .** For the optimized structures of  $\text{Mg}^+(\text{H}_2\text{O})_n$  and  $(\text{MgOH})^+(\text{H}_2\text{O})_{n-1}$ , the hydration energies and reaction energies (internal energy change) of  $\text{Mg}^+(\text{H}_2\text{O})_n$  are evaluated. The hydration energies of  $\text{Mg}^+(\text{H}_2\text{O})_n$  and  $(\text{MgOH})^+(\text{H}_2\text{O})_{n-1}$  are defined in the following reactions:



and



and the corresponding internal energy changes are

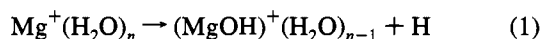
$$\Delta E(n) = E(n) - \{E(n-1) + E(\text{H}_2\text{O})\}$$

and

$$\Delta E'(n) = E'(n) - \{E'(n-1) + E(\text{H}_2\text{O})\}$$

where  $\Delta E(n)$  and  $\Delta E'(n)$  are the hydration energies of  $\text{Mg}^+(\text{H}_2\text{O})_n$  and  $(\text{MgOH})^+(\text{H}_2\text{O})_n$ ,  $E(n)$  and  $E'(n)$  are the total energies of  $\text{Mg}^+(\text{H}_2\text{O})_n$  and  $(\text{MgOH})^+(\text{H}_2\text{O})_n$ , respectively, and  $E(\text{H}_2\text{O})$  is the total energy of an  $\text{H}_2\text{O}$ .

The hydrogen elimination reaction is



and its internal energy change  $D(n)$  is given by

$$D(n) = E(n) - \{E'(n-1) + E(\text{H})\}$$

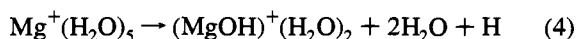
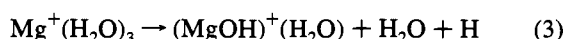
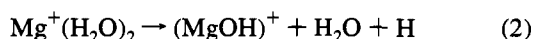
where  $E(\text{H})$  is the total energy of a hydrogen atom.

These energies are evaluated by the MP2//SCF and MP4SDTQ//SCF methods with 6-31G and 6-31G\* basis sets. The structures used for these evaluations are the most stable isomers for each  $n$ . Table 4 shows the hydration energies of  $\text{Mg}^+(\text{H}_2\text{O})_n$  ( $-\Delta E(n)$ ) and  $(\text{MgOH})^+(\text{H}_2\text{O})_{n-1}$  ( $-\Delta E'(n)$ ). In both  $\text{Mg}^+(\text{H}_2\text{O})_n$  and  $(\text{MgOH})^+(\text{H}_2\text{O})_{n-1}$ , the hydration energies are nonadditive.

Table 5 shows the hydrogen elimination energies of  $\text{Mg}^+(\text{H}_2\text{O})_n$  ( $-D(n)$ ). The energies are evaluated also with MP2//SCF and MP4SDTQ//SCF methods in the two basis sets. The hydrogen elimination energy for  $n = 1$ ,  $-D(1)$ , is as large as 3.3 eV in all calculation levels, but  $-D(n)$  become smaller as the cluster size  $n$  increases. As is discussed above, the magnesium atom in  $(\text{MgOH})^+$  nearly oxidized to  $\text{Mg}^{1.5+}$ . Thus, the hydration energy  $\Delta E'(n)$  is much larger than  $\Delta E(n)$  for a fixed  $n$ . Consequently, the energy difference between  $E'(4) + E(\text{H})$  and  $E(5)$  is very small. And, at last,  $-D(6)$  becomes negative; in other words,  $(\text{MgOH})^+(\text{H}_2\text{O})_5 + \text{H}$  is more stable than  $\text{Mg}^+(\text{H}_2\text{O})_6$ . The sign change of  $D(n)$  at  $n = 6$  is consistent with the product switch reported in the preceding paper.<sup>31</sup> The products of the hydrogen elimination reaction,  $(\text{MgOH})^+(\text{H}_2\text{O})_{n-1}$ , become dominant for  $n \geq 6$  in the TOF mass spectra of  $\text{Mg}^+$ -water clusters.

**Correction of the Zero-Point Vibrational Energies.** The qualitative change of the main peak of the TOF mass spectrum can be explained with the internal energy changes  $-\Delta E(n)$  and  $-\Delta E'(n)$  and  $-D(n)$ . To discuss it more quantitatively, the zero-point vibrational energies are to be taken into account. The internal energy changes with corrections of the zero-point vibrational energies of  $\text{Mg}^+(\text{H}_2\text{O})_n$  ( $-\Delta E_{\text{zpv}}(n)$ ) and  $(\text{MgOH})^+(\text{H}_2\text{O})_n$  ( $-\Delta E'_{\text{zpv}}(n)$ ) and the hydrogen elimination energies ( $-D_{\text{zpv}}(n)$ ) are shown in Tables 6 and 7. Total energies of  $\text{Mg}^+(\text{H}_2\text{O})_n$  ( $-\Delta E(n)$ ) and  $(\text{MgOH})^+(\text{H}_2\text{O})_n$  ( $-\Delta E'(n)$ ) are evaluated at MP4SDTQ//SCF and MP2//SCF levels, and the zero-point vibrational energies are evaluated at SCF//SCF levels. Basis sets used are 6-31G and 6-31G\*. Figure 7 shows the energy diagrams of the hydration and hydrogen elimination energies with the zero-point vibrational energies corrections using the 6-31G\* basis set.

The dissociation energies of the following reactions are deduced from the photofragment ion mass spectra in the preceding paper.<sup>31</sup> In the experiments, the energies of reaction 2, 3, and 4 are deduced to be 3.60, 2.82, and 2.43 eV,



respectively. In our calculations, the dissociation energy of reaction 2 without the zero-point vibrational energy is  $-\{D(1)$

**Table 4.** Hydration Energy for  $\text{Mg}^+(\text{H}_2\text{O})_n$  ( $-\Delta E(n)/\text{eV}$ ) and  $(\text{MgOH})^+(\text{H}_2\text{O})_n$  ( $-\Delta E'(n)/\text{eV}$ )

		6-31G*		6-31G	
		MP4SDTQ//SCF	MP2//SCF	MP4SDTQ//SCF	MP2//SCF
$\text{Mg}^+(\text{H}_2\text{O})_n$	$-\Delta E(1)$	1.727	1.725	1.925	1.929
	$-\Delta E(2)$	1.447	1.444	1.625	1.626
	$-\Delta E(3)$	1.273	1.269	1.399	1.396
	$-\Delta E(4)$	0.939	0.951	1.108	1.114
	$-\Delta E(5)$	0.826	0.838	0.971	0.977
	$-\Delta E(6)$		0.631	0.811	0.836
$(\text{MgOH})^+(\text{H}_2\text{O})_n$	$-\Delta E'(1)$	2.562	2.572	2.831	2.851
	$-\Delta E'(2)$	2.005	2.008	2.272	2.286
	$-\Delta E'(3)$	1.666	1.682	1.797	1.797
	$-\Delta E'(4)$	1.206	1.209	1.368	1.370
	$-\Delta E'(5)$	1.156	1.157	1.143	1.142

**Table 5.** Hydrogen Elimination Energy for  $\text{Mg}^+(\text{H}_2\text{O})_n$  ( $-D(n)/\text{eV}$ )

	6-31G*		6-31G	
	MP4SDTQ//SCF	MP2//SCF	MP4SDTQ//SCF	MP2//SCF
$-D(1)$	3.303	3.247	3.359	3.330
$-D(2)$	2.188	2.119	2.153	2.104
$-D(3)$	1.457	1.380	1.281	1.214
$-D(4)$	0.729	0.668	0.592	0.531
$-D(5)$	0.349	0.297	0.195	0.139
$-D(6)$		-0.229	-0.136	-0.170

**Table 6.** Hydration Energies with Zero-Point Vibration Corrections for  $\text{Mg}^+(\text{H}_2\text{O})_n$  ( $-\Delta E_{\text{zpv}}(n)/\text{eV}$ ),  $(\text{MgOH})^+(\text{H}_2\text{O})_n$  ( $-\Delta E'_{\text{zpv}}(n)/\text{eV}$ ),  $\text{Mg}^+(\text{D}_2\text{O})_n$  ( $-\Delta E_{\text{zpv}}^{\text{D}}(n)/\text{eV}$ ), and  $(\text{MgOD})^+(\text{D}_2\text{O})_n$  ( $-\Delta E'_{\text{zpv}}^{\text{D}}(n)/\text{eV}$ )

		6-31G*		6-31G	
		MP4SDTQ//SCF	MP2//SCF	MP4SDTQ//SCF	MP2//SCF
$\text{Mg}^+(\text{H}_2\text{O})_n$	$-\Delta E_{\text{zpv}}(1)$	1.654	1.653	1.817	1.821
	$-\Delta E_{\text{zpv}}(2)$	1.347	1.339	1.497	1.498
	$-\Delta E_{\text{zpv}}(3)$	1.162	1.163	1.274	1.270
	$-\Delta E_{\text{zpv}}(4)$	0.822	0.834	0.953	0.959
	$-\Delta E_{\text{zpv}}(5)$	0.698	0.710	0.812	0.818
	$-\Delta E_{\text{zpv}}(6)$		0.576	0.741	0.766
$(\text{MgOH})^+(\text{H}_2\text{O})_n$	$-\Delta E'_{\text{zpv}}(1)$	2.468	2.478	2.709	2.729
	$-\Delta E'_{\text{zpv}}(2)$	1.902	1.905	2.129	2.143
	$-\Delta E'_{\text{zpv}}(3)$	1.550	1.547	1.678	1.678
	$-\Delta E'_{\text{zpv}}(4)$	1.096	1.099	1.247	1.248
	$-\Delta E'_{\text{zpv}}(5)$	1.011	1.013	1.011	1.010
	$-\Delta E'_{\text{zpv}}(6)$		0.587	0.754	0.779
$\text{Mg}^+(\text{D}_2\text{O})_n$	$-\Delta E_{\text{zpv}}^{\text{D}}(1)$	1.666	1.665	1.837	1.841
	$-\Delta E_{\text{zpv}}^{\text{D}}(2)$	1.366	1.363	1.522	1.523
	$-\Delta E_{\text{zpv}}^{\text{D}}(3)$	1.184	1.179	1.298	1.295
	$-\Delta E_{\text{zpv}}^{\text{D}}(4)$	0.847	0.859	0.988	0.994
	$-\Delta E_{\text{zpv}}^{\text{D}}(5)$	0.726	0.739	0.849	0.854
	$-\Delta E_{\text{zpv}}^{\text{D}}(6)$		0.587	0.754	0.779
$(\text{MgOD})^+(\text{D}_2\text{O})_n$	$-\Delta E'_{\text{zpv}}^{\text{D}}(1)$	2.482	2.491	2.732	2.752
	$-\Delta E'_{\text{zpv}}^{\text{D}}(2)$	1.921	1.924	2.155	2.169
	$-\Delta E'_{\text{zpv}}^{\text{D}}(3)$	1.573	1.569	1.701	1.701
	$-\Delta E'_{\text{zpv}}^{\text{D}}(4)$	1.117	1.121	1.271	1.273
	$-\Delta E'_{\text{zpv}}^{\text{D}}(5)$	1.043	1.044	1.039	1.039
	$-\Delta E'_{\text{zpv}}^{\text{D}}(6)$		0.587	0.754	0.779

+  $\Delta E(2)\} = 3.30 + 1.45 = 4.75$  eV at the MP4SDTQ//SCF/6-31G\* level, and with the zero-point vibrational correction, it becomes  $-\{D_{\text{zpv}}(1) + \Delta E_{\text{zpv}}(2)\} = 2.95 + 1.35 = 4.30$  eV. The correction for the zero-point vibrational energy gives a better estimation, but the calculation is still far from the experimental energy. The calculated dissociation energies of

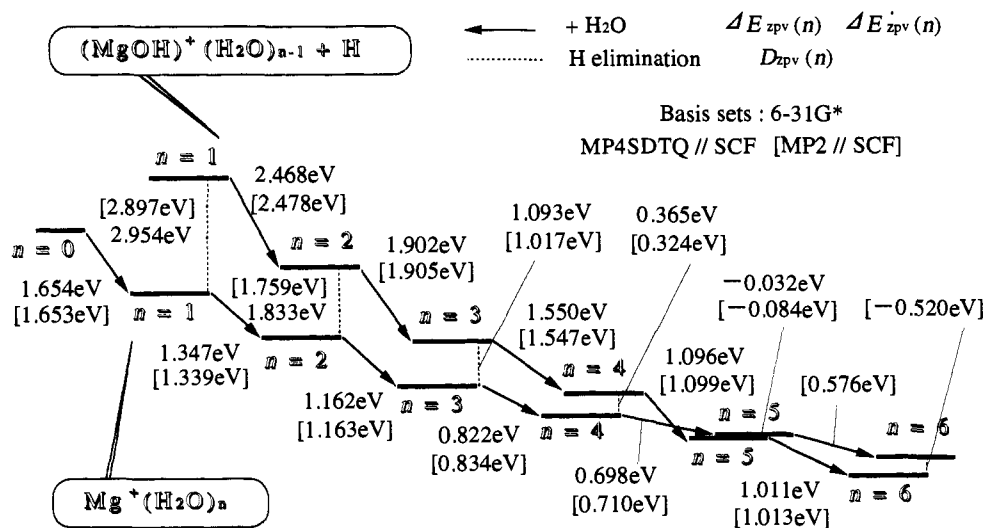


**Figure 7.** Hydration and reaction energies of  $\text{Mg}^+(\text{H}_2\text{O})_n$  with correction for the zero-point vibration energy. The dotted lines are the hydrogen elimination energies of  $\text{Mg}^+(\text{H}_2\text{O})_n$  ( $D_{zpv}(n)$ ). The arrows are the hydration energies of  $\text{Mg}^+(\text{H}_2\text{O})_n$  ( $-\Delta E_{zpv}(n)$ ) and  $\text{Mg}^+(\text{H}_2\text{O})_{n-1}$  ( $-\Delta E'_{zpv}(n)$ ).

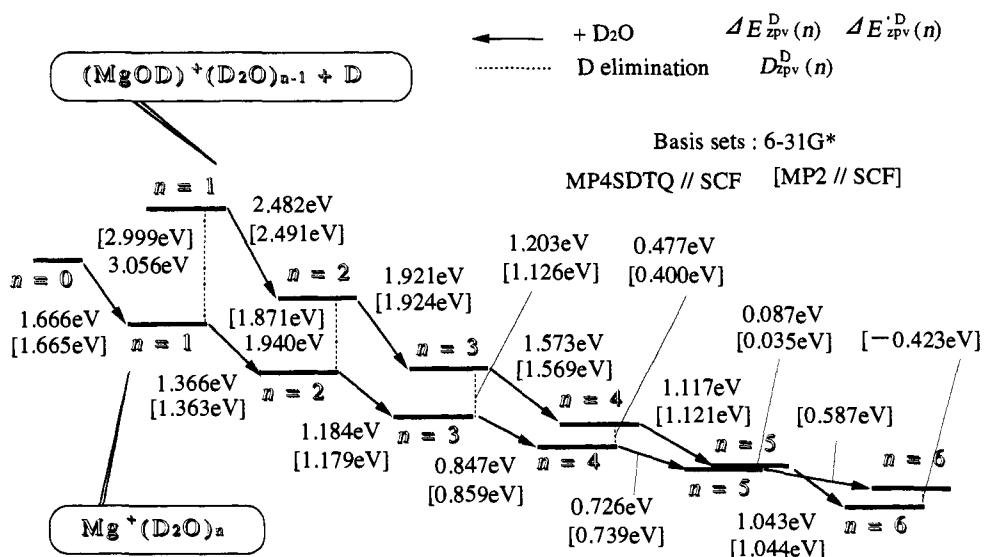


**Figure 8.** Hydration and reaction energies of  $\text{Mg}^+(\text{D}_2\text{O})_n$ . The dotted lines are the deuterium elimination energies of  $\text{Mg}^+(\text{D}_2\text{O})_n$  ( $D_{zpv}^D(n)$ ). The arrows are the hydration energies of  $\text{Mg}^+(\text{D}_2\text{O})_n$  ( $-\Delta E_{zpv}^D(n)$ ) and  $(\text{MgOD})^+(\text{D}_2\text{O})_{n-1}$  ( $-\Delta E'_{zpv}^D(n)$ ).

reactions 3 and 4 without the zero-point vibrational energies are  $-\{D(2) + \Delta E(3)\} = 2.19 + 1.27 = 3.46$  eV and  $-\{D(3) + \Delta E(4) + \Delta E(5)\} = 1.46 + 0.94 + 0.83 = 3.23$  eV, respectively, and with the zero-point vibrational energies are  $-\{D_{zpv}(2) + \Delta E_{zpv}(3)\} = 1.83 + 1.16 = 2.99$  eV and  $-\{D_{zpv}(3) + \Delta E_{zpv}(4) + \Delta E_{zpv}(5)\} = 1.09 + 0.82 + 0.69 = 2.60$  eV. The calculated energies with the zero-point vibrational energies of reactions 3 and 4 are in good agreement with the experimental results.

Bauschlicher and Partridge also evaluated the hydration energies  $-\Delta E(n)$  and  $-\Delta E_{zpv}(n)$  for  $n = 1$  and 2 with the SCF/TZ2P level of approximation.<sup>22</sup> Their values of  $-\Delta E(1)$ ,  $-\Delta E_{zpv}(1)$ ,  $-\Delta E(2)$ , and  $-\Delta E_{zpv}(2)$ , are 1.388, 1.323, 1.136, and 1.049 eV, respectively, which are almost uniformly smaller by 0.3 eV than our corresponding values shown in Table 4 and Figure 7.

Misaizu, Fuke, and their co-workers deduced that the binding energies of  $(\text{MgOH})^+(\text{H}_2\text{O})$  and  $(\text{MgOH})^+(\text{H}_2\text{O})_2$  are 1.9 and 1.5 eV, respectively.<sup>30</sup> In our calculations, these energies are 2.56 eV ( $\Delta E'(1)$ ) and 2.01 eV ( $\Delta E'(2)$ ) without the zero-point vibrational correction and 2.47 eV ( $\Delta E'_{zpv}(1)$ ) and 1.90 eV ( $\Delta E'_{zpv}(2)$ ) at the MP4SDTQ//SCF/6-31G\* level.

The zero-point vibration correction reduces the discrepancy between our theoretical and experimentally estimated values by 0.1 eV, but there remains a substantial discrepancy, particularly for  $n = 1$ , the cause of which might be the basis set deficiency in our calculation or the error in the experimental evaluation.

**The First Product Switching.** In the preceding paper, the deuterium effect on the product distribution of  $\text{Mg}^+(\text{D}_2\text{O})_n$  and  $(\text{MgOD})^+(\text{D}_2\text{O})_{n-1}$  is studied.<sup>31</sup> The calculated energy changes  $\Delta E_{zpv}^D(n)$  and  $\Delta E'_{zpv}^D(n)$  and  $D_{zpv}^D(n)$  for  $\text{Mg}^+(\text{D}_2\text{O})_n$  and  $(\text{MgOD})^+(\text{D}_2\text{O})_{n-1}$  are shown in Tables 6 and 7.

Experimentally, the product of the deuterium elimination reaction starts to dominate at  $n = 6$ .<sup>31</sup> In the calculations, the elimination reaction energy  $D_{zpv}^D(n)$  is negative at  $n = 5$  with the 6-31G set and at  $n = 6$  with the 6-31G\* set (see Tables 6 and 7). The calculated deuterium elimination energies  $D_{zpv}^D(n)$  are always larger than the corresponding hydrogen elimination energies  $D_{zpv}(n)$  (compare Figures 7 and 8) because the zero-point vibrational correction is smaller for the deuterium system. If the harmonic frequencies are assumed, the partition functions of the reactants and products are known and, thus, the equilibrium constants  $K_p(n)$  and  $K_p^D(n)$  can be evaluated for



**Table 7.** Hydrogen Elimination Energies Corrected with Zero-Point Vibrational Energies for  $\text{Mg}^+(\text{H}_2\text{O})_n$  ( $-D_{\text{zpv}}(n)/\text{eV}$ ) and  $\text{Mg}^+(\text{D}_2\text{O})_n$  ( $-D_{\text{zpv}}^{\text{D}}(n)/\text{eV}$ )<sup>a</sup>

		6-31G*		6-31G	
		MP4SDTQ//SCF	MP2//SCF	MP4SDTQ//SCF	MP2//SCF
$\text{Mg}^+(\text{H}_2\text{O})_n$	$-D_{\text{zpv}}(1)$	2.954	2.897	3.037	3.008
	$-D_{\text{zpv}}(2)$	1.833	1.759	1.826	1.776
	$-D_{\text{zpv}}(3)$	1.093	1.017	0.970	0.904
	$-D_{\text{zpv}}(4)$	0.365	0.304	0.245	0.184
	$-D_{\text{zpv}}(5)$	-0.032	-0.084	-0.189	-0.245
	$-D_{\text{zpv}}(6)$		-0.520	-0.458	-0.490
$\text{Mg}^+(\text{D}_2\text{O})_n$	$-D_{\text{zpv}}^{\text{D}}(1)$	3.056	2.999	3.133	3.104
	$-D_{\text{zpv}}^{\text{D}}(2)$	1.940	1.871	1.924	1.875
	$-D_{\text{zpv}}^{\text{D}}(3)$	1.203	1.126	1.067	1.000
	$-D_{\text{zpv}}^{\text{D}}(4)$	0.477	0.400	0.354	0.293
	$-D_{\text{zpv}}^{\text{D}}(5)$	0.087	0.035	-0.069	-0.126
	$-D_{\text{zpv}}^{\text{D}}(6)$		-0.423	-0.355	-0.386

<sup>a</sup> Values are in electronvolts.

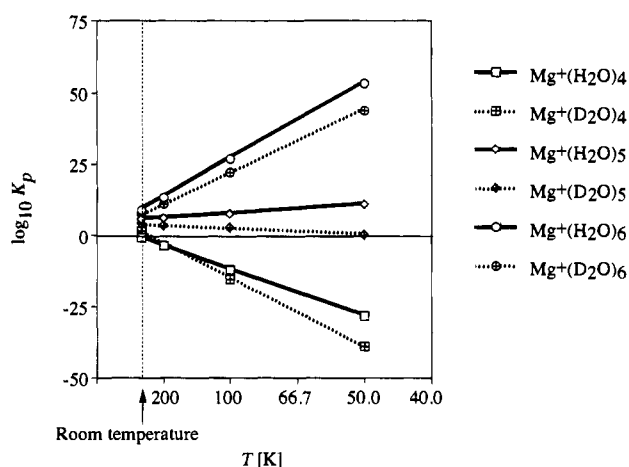


**Figure 9.** Logarithm plots of the equilibrium constants  $K_p(n)$  and  $K_p^{\text{D}}(n)$  of reaction 1 against  $1/T$ . The positive  $\log_{10} K_p$  implies that the elimination product is dominant.

the following reactions:

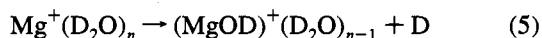


Figure 9 shows the sizes and temperature dependencies of  $\log_{10} K_p(n)$  and  $\log_{10} K_p^{\text{D}}(n)$ . The pressure is 1.0 atm. The basis set used is 6-31G\*. The positive  $\log_{10} K_p$  implies that the elimination product is dominant. In the TOF spectra in the preceding paper,<sup>31</sup> the main products start to change to hydrogen (deuterium-) eliminated clusters at  $n = 5$  in  $\text{Mg}^+-\text{H}_2\text{O}$  and at  $n = 6$  in the  $\text{Mg}^+-\text{D}_2\text{O}$  system.<sup>31</sup> When deuterium is substituted for hydrogen, the equilibrium moves to the reactant.

The calculated equilibrium constants can explain the feature of the TOF spectrum for the deuterium effect. Under lower temperature, the switching cluster size shifts to larger  $n$ . It should be noted that the experiments were carried out under a supersonic beam condition; the actual temperature is unknown, and in reality, usually it is not thermally in equilibrium. The rotational temperature is in most cases very low, but the internal vibrational temperature, which is more important in chemical reactions in clusters, is not as low as the rotational temperature. Thus, our calculations of the equilibrium constants, their temperature dependencies, and the isotope effects are consistent with experimental findings.

Harms et al. also examined the product switching with their ab initio calculations, but they used the reaction



instead of eq 1 and found a sign change in the energy difference between  $n = 3$  and  $n = 4$ .<sup>15</sup>

### Conclusions and Future Studies

The difference in the internal energies of the reactants and products explains the observed first product switching of the main TOF spectrum from  $\text{Mg}^+(\text{H}_2\text{O})_n$  to  $(\text{MgOH})^+(\text{H}_2\text{O})_{n-1}$ . The reaction is the hydrogen elimination of a water molecule, and it is also regarded as the oxidation reaction of  $\text{Mg}^+$ . From the inorganic chemical point of view, it should be emphasized that the oxidation–reduction reaction takes place in such a small cluster as  $\text{Mg}^+(\text{H}_2\text{O})_6$ . Experimentally, for  $n \geq 15$ , the reswitching to  $\text{Mg}^+(\text{H}_2\text{O})_n$  in the TOF spectrum is found. In the preceding paper,<sup>31</sup> three candidates are presented for the product of this second switching. The first candidate is the product of the insertion reaction  $(\text{HMgOH})^+(\text{H}_2\text{O})_{n-1}$ , but this reaction was ruled out because it is energetically unfavored. The second candidate was a Rydberg-type ion pair state,  $[\text{Mg}^{2+}(\text{H}_2\text{O})_n]^-$ ; because of the closed shell nature of  $\text{Mg}^{2+}$ , the reaction of  $\text{Mg}^{2+}$  with a water molecule is suppressed. The third candidate was the product of further a oxidation–reduction reaction such as  $\text{MgOH}(\text{H}_3\text{O}^+)(\text{H}_2\text{O})_{n-2}$ . In fact, very recently,<sup>35</sup> during the study of a boron ion  $\text{B}^+$  cluster with water molecules, we found that the most stable isomer is  $\text{BOH}(\text{HOH}_2^+)$ ; a proton is spontaneously transferred to a water molecule to form an oxonium ion  $\text{OH}_3^+$ . If a similar reaction takes place in the  $\text{Mg}^+$  clusters, we should apparently observe  $[\text{Mg}(\text{H}_2\text{O})_n]^+$  in the TOF spectrum, though the reaction actually proceeds in the cluster.

To elucidate the second switching, more work is required both experimentally and theoretically.

**Acknowledgment.** The authors thank Dr. Sanekata for discussion. A part of the work was supported by the Grant-in-Aids for Scientific Research (No. 04640458) and for Priority Area (No. 04243102) by the Ministry of Education, Science and Culture, Japan. This work was supported by the Joint Studies Program (1994) of the Institute for Molecular Science.

JA942521Q